Available online at www.sciencedirect.com
ScienceDirect
Surface & Coatings Technology 201 (2007) 5358–5362
SURFACE & COATINGS TECHNOLOGY
www.elsevier.com/locate/surfcoat

Top-emitting organic light-emitting diode using transparent conducting indium oxide layer fabricated by a two-step ion beam-assisted deposition

J.T. Lim, C.H. Jeong, A. Vozny, J.H. Lee, M.S. Kim, G.Y. Yeom *

Department of Materials Science and Engineering, Sungkyunkwan University, Suwon 440-746, Korea, Republic of Korea

Available online 14 August 2006

Abstract

To fabricate the top-emitting organic light-emitting diodes (TEOLEDs) with an improved device performance, an n-type indium oxide (IO) was deposited as the transparent conducting capping layer, by using ion beam-assisted deposition (IBAD) technique, on the device of glass/Ag (100 nm)/ITO (100 nm)/2-TNATA (60 nm)/NPB (20 nm)/Alq_3 (40 nm)/LiF (1 nm)/Al (2 nm)/Ag (20 nm), and its properties were investigated. To minimize the damage to the organic layers and the oxidation of the top Ag layer during the oxygen IBAD, two-step processing of IO thin film composed of argon IBAD followed by oxygen IBAD was used. The light output of TEOLED fabricated by using the IBAD was similar compared with that of a reference device composed of glass/Ag (100 nm)/ITO (100 nm)/2-TNATA (60 nm)/NPB (20 nm)/Alq_3 (40 nm)/LiF (1 nm)/Al (2 nm)/Ag (20 nm)/Alq_3 (52 nm), where, Alq_3 was used as the semi-passivated capping layer.
© 2006 Elsevier B.V. All rights reserved.

PACS: 81.15.J; 72.80.L
Keywords: IBAD; Organic semiconductors; Top emission; TEOLED; IO; Buffer layer

1. Introduction

Top-emitting organic light-emitting diode (TEOLED) devices have been actively studied for their applications in active-matrix displays with a high aperture ratio, because of their geometrical merit allowing a high pixel resolution [1,2]. To improve the TEOLED performance, transparent conducting oxides (TCO) such as indium oxide (IO), tin oxide, zinc oxide, etc. [3–5], which must have high transparency as well as low resistance, need to be deposited on the top of the devices as the capping cathode layer, and it is important to reduce damage occurring during the deposition of the TCO layer.

To reduce the damage during the deposition of TCO layer, transparent or semi-transparent conducting buffer layers such as MgAg [6,7], CuPc [8], Li/CuPc [9], Li doped BPhen [10], Ca and/or LiF/Al [11], 3,4,9,10-perlyenetetracarboxylic dianhydride [8], metal acetylacetonate complexes [12], and pentacene [13] are generally deposited on the device before the deposition of the TCO layer. Even though the addition of such buffer layers could reduce high energetic plasma damage during the TCO deposition such as sputter deposition, it is not easy to completely avoid plasma damage because of the high sensitivity of organic films to radiation, charging, and heating. Especially, during the conventional sputter deposition processing, energetic particles, such as reflected neutrons, high energy γ electrons, and charged ions attack the surface of organic layers and transfer their high energies to the organic layers [14]. These result in the degradation of an underlying organic layers and/or a buffer layer such as Al and Ag, induced by oxygen ions during the sputter deposition of the oxides. It is essential to find a way of minimizing the damage caused by the sputtering deposition of TCO films.

In this work, to reduce the physical damage of organic layers and oxidation of buffer layers occurring by oxygen plasma during the IO deposition by oxygen ion beam-assisted evaporation, a two-step IO deposition process consisted of argon ion beam-assisted deposition (IBAD) of IO followed by oxygen IBAD of IO was utilized. The physical and electrical properties of the IBAD-grown IO thin film were investigated and the current density–voltage–luminance curves of the TEOLED device having the IO capping layer deposited by the two-step IBAD process were characterized.

* Corresponding author.
E-mail address: gyyeom@skku.edu (G.Y. Yeom).

0257-8972/$ - see front matter © 2006 Elsevier B.V. All rights reserved.
doi:10.1016/j.surfcoat.2006.07.036

2. Experimental details

2.1. Fabrication of TEOLED

All organic layers, lithium fluoride, and the Al/Ag buffer cathode layer composing of TEOLED were fabricated by vacuum evaporation and the Ag anode layer and the SiO_2 edge-passivation layer, which prevents short circuit between the top cathode layer and the bottom anode layer during the TCO deposition, were deposited by using electron beam evaporation. Also, the ITO layer composing the anode was fabricated by dc sputtering followed by a heat treatment. Fig. 1 exhibits the schematic diagram of the device structure for Device 1, in which IO as the capping layer was deposited on the device structure of glass/Ag (100 nm)/ITO (about 20–30 Ω/□)/2-TNATA (60 nm)/NPB (20 nm)/Alq_3 (40 nm)/LiF (1 nm)/Al (2 nm)/Ag (20 nm). Device 2 was fabricated as a reference device, in which the semi-passivated capping layer of tris[8-hydroxyquinolinonato]aluminum (III) (Alq_3) was deposited on the above structure instead of IO. In the layers for TEOLEDs, 4,4′,4”-tris[2-naphthylphenyl-1-phenylamino]triphenylamine (2-TNATA) was used as a hole-injecting layer (HIL), 4,4′-bis[*N*-(1-napthyl)-*N*-phenyl-amino]-biphenyl (NPB) as a hole-transporting layer (HTL), Alq_3 as ETL, and lithium fluoride (LiF) as an electron-injecting layer (EIL), aluminum (2 nm)/silver (20 nm) as a buffer electrode layer to reduce the damage to the organic layers during the IO deposition. The emissive active area of the devices was 2 mm × 2 mm.

2.2. Deposition of the IO capping layer by IBAD system

The IO thin film deposition was conducted using an IBAD system. The IBAD system was consisted of an electron beam evaporator for the evaporation of IO and an internally mounted inductively coupled ion gun for the supply of argon or oxygen ions to the substrate. The ion gun was driven by an rf inductively coupled plasma of 13.56 MHz. Also, two grids were used to efficiently extract and accelerate the generated ions and were insulated by ceramics located between them. The ion gun of the IBAD system was facing the substrate holder at an angle of 30–40° to the surface normal of the substrate to reduce the physical damage to the substrate.

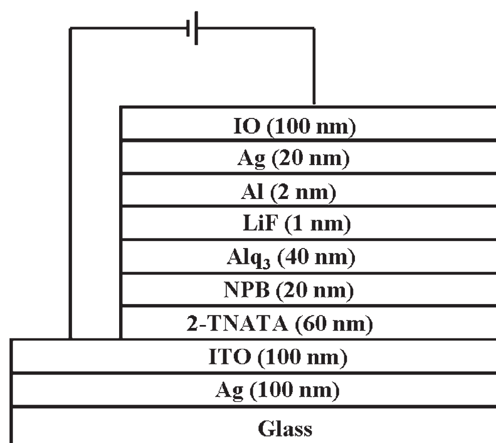

Fig. 1. The schematic diagram for the TEOLED device (Device 1) with IO deposited by a two-step IBAD.

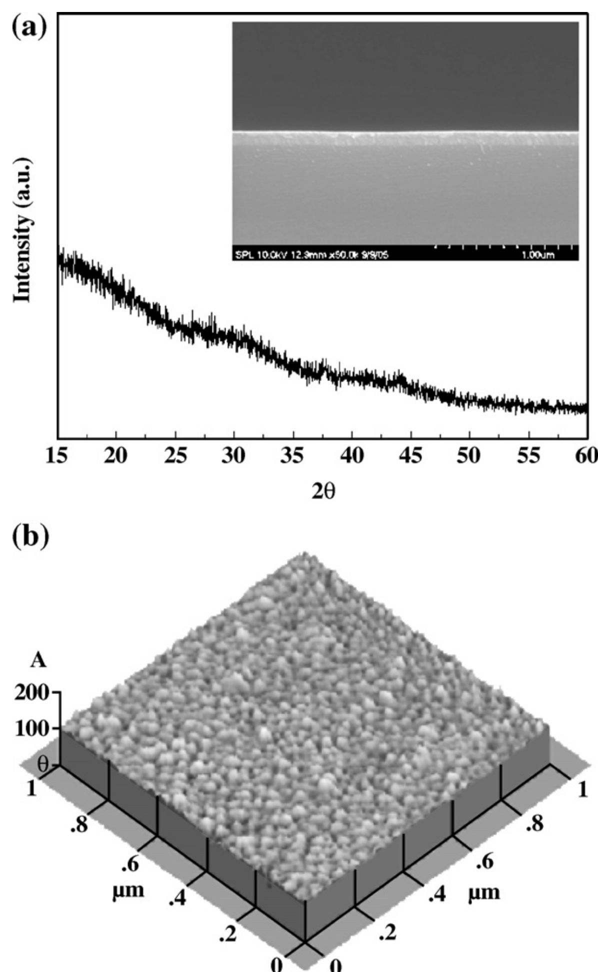

Fig. 2. (a) XRD plot of the IO cathode layer deposited by two-step IBAD composed of argon IBAD (5 nm) followed by oxygen IBAD (95 nm). Insert: the cross-sectional SEM image of the IO thin film. (b) AFM image of the IO thin film.

The IO thin film deposition was carried out in two-steps at room temperature, that is, first, the deposition of IO film by electron beam evaporation with Ar ion beam irradiation, and next, the IO film deposition by electron beam evaporation with oxygen ion beam irradiation. For the Ar ion assisted deposition of IO, the Ar ion gun was operated at the rf power of 250 W, +60 V to the acceleration grid, and 0 V to the extraction grid while flowing the Ar gas at 10 sccm to the ion gun. In the case of oxygen ion assisted evaporation, the ion gun was operated at rf powers of 250 W, +300 V to the acceleration grid, and 0 V to the extraction grid while flowing the oxygen gas at 17 sccm to the ion gun. The deposition rates of the IO using argon IBAD and oxygen IBAD were 0.02 nm/s and 0.06 nm/s, respectively. The source for the electron beam evaporation of IO was a pellet of IO with 99.99% purity (PURE TECH Co. Ltd.).

2.3. General measurements

The reflectance spectrum of glass/Al/ITO anode and transmittance spectrum of the deposited Al/Ag/IO cathode layer were

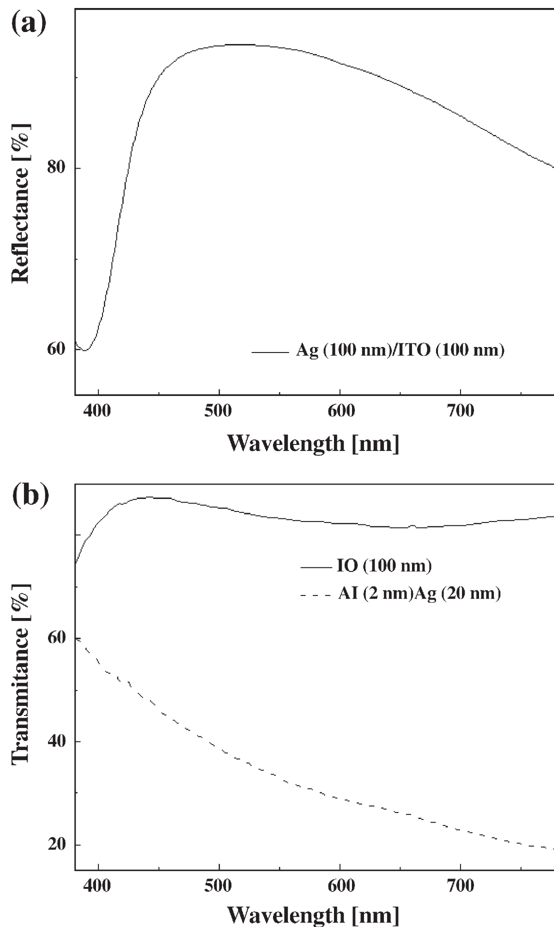

Fig. 3. (a) Reflection spectrum of the anode composed of Ag (100 nm)/ITO (100 nm). (b) Transmittance spectra of the 100-nm-thick IO film deposited by the two-step IBAD and Al (2 nm)/Ag (20 nm) film.

measured by using a UV–VIS-NIR Spectrophotometer attached with VW specular wavelength reflectance (Cary 5000 UV/VIS/NIR, Varian Inc.) and a UV spectrophotometer (UV S-2100, SCINCO Inc.), respectively. The resistivity was measured by a four-point probe (CMT-SERIES, CHANG MIN Co. Ltd.).

The microstructure of the IO film deposited by the IBAD system was measured by a high resolution multi-purpose X-ray diffractometer (HRXRD) with Cu $K_{\alpha 1}$ (1.54 Å) (D8 Discover, Bruker AXS Ltd.). The surface morphology of the IO film was measured by scanning electron microscope (SEM) (S-4700, Hitachi, Ltd.) and atomic force microscopy (AFM) (CP Research, THERO-MICROSCOPES, Ltd.).

Current-voltage characteristics were measured with a source-measure unit (236, Keithley Instruments, Inc.). The intensities from the blue emission of the devices were measured by the photocurrent induced on the silicon photodiodes using a picoammeter (485, Keithley Instruments, Inc.). The electroluminescent spectra of the fabricated blue devices were measured by optical emission spectroscopy (PCM-420, SC Tech. Inc.).

3. Results and discussion

The device configuration of TEOLED as shown in Fig. 1 is glass/Ag (100 nm)/ITO (100 nm)/2-TNATA (60 nm)/NPB (20 nm)/Alq_3 (40 nm)/LiF (1 nm)/Al (2 nm)/Ag (20 nm)/IO (100 nm). Among these layers, the buffer layer of Al (2 nm)/Ag (20 nm) plays an important role, such as protecting the organic layers from the energetic particles, electrical charging, heat, light, etc. that is occurred during the deposition of IO by IBAD. Efficient electron injection from a cathode into the Alq_3 layer can be obtained when the work function of a cathode is similar to the electron affinity of the Alq_3 layer and an efficient injection closely depends on the work function of LiF/Al in the TEOLED structure. In our TEOLED structure, 2 nm thick Al layer composing of the buffer layer is expected to exhibit an efficient electron-injecting ability. Hung et al. proved that a LiF/Al bilayer with the Al layer as thin as 0.1 nm is sufficient to form an effective electron-injecting contact to the Alq_3 by comparing turn-on voltages and luminous efficiencies as a function of the LiF thickness on a glass/ITO/NPB/Alq_3/LiF/Al/Ag device [15]. Meanwhile, the Ag layer in the Al/Ag buffer layer was used to prevent oxidation of the Al layer from moisture and oxygen. However, the Ag layer was found to be easily oxidized during the deposition of IO using oxygen IBAD. To prevent the oxidation of Ag of the Al/Ag buffer layer, the deposition of the IO film was carried out in two-steps. First, by flowing 10 sccm of argon to the ion gun instead of oxygen, 5-nm-thick initial IO buffer layer was deposited at a low ion energy of

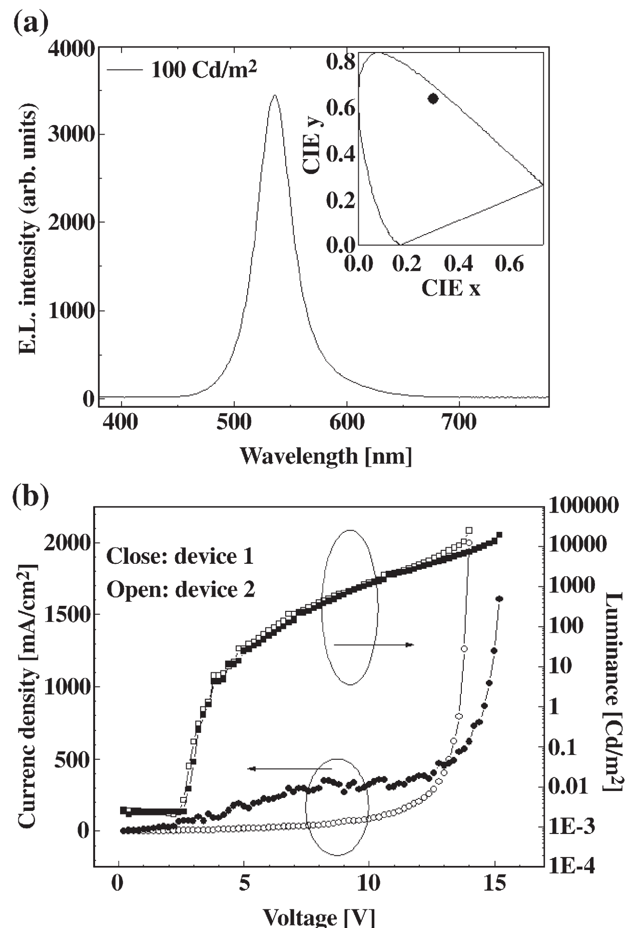

Fig. 4. (a) EL spectrum of Device 1 at a luminance of about 100 Cd/m². Insert: the CIE co-ordinate of Device 1 at the normal viewing angle. (b) Current density–voltage–luminance characteristics of Devices 1 and 2.

~60 eV. The Al (2 nm)/Ag (20 nm)/ IO (5 nm) layer showed a sheet resistance of about 5 Ω/□. Second, by using oxygen IBAD, the remaining 95 nm thick IO film was deposited. The resistivity of the IO deposited by oxygen IBAD was less than 5×10^{-4} Ω·cm. Therefore, using this two-step deposition of the IO film, the oxidation of the Ag surface was successfully suppressed while keeping low resistivity of IO.

The physical characteristics of the 100 nm thick IO film deposited by the above two-step IBAD were investigated by XRD, cross-sectional SEM, and AFM. Fig. 2(a) shows the XRD plot of the IO and the insert of Fig. 2 exhibits a cross-sectional SEM image of the IO. As shown in the figure, the IO film deposited by the two-step IBAD showed the characteristic of amorphous structure with no peaks. In general, when IO was deposited by a conventional dc magnetron sputtering, a typical polycrystalline structure with a columnar grain is obtained with the grain size of about 100 Å [16]. However, in the case of the IO deposited by IBAD, as shown in the insert of Fig. 2, no columnar grain was observed and amorphous film was obtained as shown in Fig. 2 possibly due to the oxygen ion assist during the IO deposition. In addition, as shown in the AFM image of Fig. 2(b), due to the amorphous phase, the deposited IO film was very smooth with a root-mean-square (rms) roughness of 5.4 Å.

The TEOLED structure requires a high aperture ratio and it can be obtained by using a highly reflective and low resistive anode (that is, Al/ITO) in addition to a highly transmittable and low resistive cathode (that is, thin Al/Ag with thick IO) as shown in Fig. 1. Fig. 3(a) shows the reflection spectrum of the Ag (100 nm)/ITO (100 nm) anode layer employed in Devices 1 and 2. The Ag/ITO anode layer, where 100 nm thick sputtered ITO was used to obtain the maximum electroluminescent (EL) output, retains a reflectivity of 87% at the wavelength range from about 440 nm to about 650 nm. Fig. 3(b) exhibits the transmittance spectra the IO cathode capping layer deposited by the two-step IBAD and the semi-transparent Al (2 nm)/Ag (20 nm) buffer layer. As shown in the figure, the IO film and the Al(2 nm)/Ag(20 nm) buffer layer showed the transparency of 84% and 34% at the wavelength of 535 nm, respectively.

Fig. 4(a) shows the EL spectrum of Device 1 emitting from the top of the device. The EL spectrum was measured at the normal viewing angle and at the luminance density of 100 Cd/m^2. As shown in the figure, the maximum EL wavelength was found to be 535 nm in Device 1. When a conventional bottom emitting OLED device which is composed of glass/ITO (120 nm)/2-TNATA (60 nm)/NPB (20 nm)/Alq_3 (40 nm)/LiF (1 nm)/Al (100 nm) was fabricated, it showed the maximum EL wavelength at 527 nm (not shown). The differences in the EL maximum wavelength between the top-emitting Device 1 and the bottom emitting OLED from the glass surface could be attributed to optical out-coupling properties such as the wide-angle and multiple-beam interference leading to the microcavity effects [17]. This interference effect is caused by the differences in the reflectivity between the Al/Ag/IO cathode layer and the Ag/ITO anode layer. Consequently, the Commission Internationale de L'Eclairage (CIE) chromaticity co-ordinate measured at the luminance density of 100 Cd/m^2 for the Device 1 was (0.300, 0.637).

Fig. 4(b) exhibits the current density–voltage–luminance characteristics of Devices 1 having IO deposited by the two-step IBAD and Device 2 having Alq_3 instead of IO for the cathode of TEOLED structures. The optical light output of Device 1 exhibited the similar maximum luminance (L_{max}) of 19,600 Cd/m^2 (at J=1.6 A/cm^2) compared with that of Device 2 (L_{max}=24,800 Cd/m^2 at J=2.0 A/cm^2) even though the leakage current of Devices 1 was measured to be a little higher than that of Device 2 with the Alq_3 in the low voltage range, and it requires more investigation. Also, the optical out-coupling efficiencies obtained were similar each other. Therefore, in this study, TEOLED device using transparent conducting oxide could be successfully fabricated using IO deposited by a two-step IBAD with a thin Al/Ag buffer layer.

4. Conclusion

A transparent conducting IO film was deposited on a TEOLED device composed of glass/AG (100 nm)/ITO (100 nm)/2-TNATA (60 nm)/NPB (20 nm)/Alq_3 (40 nm)/LiF (1 nm)/Al (2 nm)/Ag (20 nm) by using an IBAD process. To reduce damage to organic layers of the TEOLED device and to prevent oxidation of a transparent Al/Ag buffer layer, a two-step deposition of the IO thin film composed of 5 nm thick IO deposition by using argon ion beam-assisted evaporation followed by 95 nm thick IO deposition by using oxygen ion beam-assisted evaporation was used. With this two-step deposition of the IO film, the IO film exhibiting amorphous morphology with the rms roughness of 5.4 Å could be obtained with a low resistivity of 5×10^{-4} Ω cm and a transmittance of 84%, The TEOLED device with the IO layer showed a high luminance of about 20,000 Cd/m^2 similar to a reference device with the Alq_3 capping layer which does not have damage on the device.

Acknowledgments

This work was supported by the National Research Laboratory Program (NRL) of the Ministry of Science and Technology, and by the Ministry of Commerce, Industry and Energy (MOCIE). This work was supported by Sungkyunkwan University (2005).

References

[1] G. Gu, G. Parthasarathy, P.E. Burrows, P. Tian, I.G. Hill, A. Khan, S.R. Forrest, J. Appl. Phys. 86 (1999) 4067.
[2] G. Parthasarathy, C. Adachi, P.E. Burrows, S.R. Forrest, Appl. Phys. Lett. 76 (2000) 2128.
[3] T. Minami, MRS Bull. (2000) 38.
[4] A.J. Freeman, K.R. Poeppelmeier, T.O. Mason, R.P.H. Chang, T.J. Marks, MRS Bull. (2000) 45.
[5] K.L. Chopra, S. Major, D.K. Pandya, Thin Solid Films 102 (1983) 1.
[6] G. Gu, V. Bulovic, P.E. Burrows, S.R. Forrest, M.E. Thompson, Appl. Phys. Lett. 68 (1996) 2606.
[7] V. Bulovic, G. Gu, D.E. Burrows, M.E. Thompson, S.R. Forrest, Nature (Lond.) 380 (1996) 29.
[8] G. Parthasarathy, P.E. Burrows, V. Khalfin, V.G. Kozlov, S.R. Forrest, Appl. Phys. Lett. 72 (1998) 2138.

[9] L.S. Hung, C.W. Tang, Appl. Phys. Lett. 74 (1999) 3209.
[10] G. Parthasarathy, C. Adachi, P.E. Burrows, S.R. Forrest, Appl. Phys. Lett. 76 (2000) 2128.
[11] P.E. Burrows, G. Gu, S.R. Forrest, E.P. Vicenzi, T.X. Zhou, J. Appl. Phys. 87 (2000) 3080.
[12] A. Yamamori, S. Hayashi, T. Koyama, Y. Taniguchi, Appl. Phys. Lett. 78 (2001) 3343.
[13] T. Dobbertin, M. Kroeger, D. Meithecker, D. Schneider, D. Metzdouf, H. Neuner, E. Becker, H.-H. Johannes, W. Kowalsky, Appl. Phys. Lett. 82 (2003) 284.
[14] D.M. Mattox, J. Vac. Sci. Technol., A, Vac. Surf. Films 7 (1989) 1105.
[15] L.S. Hung, C.W. Tang, M.G. Mason, P. Raychandhuri, J. Madathil, Appl. Phys. Lett. 78 (2001) 544.
[16] H.W. Muller, Phys. Status Solidi 27 (1968) 723.
[17] H. Riel, S. Karg, T. Beierlein, W. Reib, J. Appl. Phys. 94 (2003) 5290.